PHILOSOPHICAL TRANSACTIONS A

rsta.royalsocietypublishing.org

Research

Cite this article: Slovick BA, Zhou Y, Yu ZG, Kravchenko II, Briggs DP, Moitra P, Krishnamurthy S, Valentine J. 2017 Metasurface polarization splitter. *Phil. Trans. R. Soc. A* **375**: 20160072.
http://dx.doi.org/10.1098/rsta.2016.0072

Accepted: 12 December 2016

One contribution of 15 to a theme issue 'New horizons for nanophotonics'.

Subject Areas:
optics, nanotechnology, materials science

Keywords:
metamaterials, metasurfaces, all-dielectric

Author for correspondence:
Brian A. Slovick
e-mail: brian.slovick@sri.com

Electronic supplementary material is available online at https://dx.doi.org/10.6084/m9.figshare.c.3668845

THE ROYAL SOCIETY PUBLISHING

Metasurface polarization splitter

Brian A. Slovick[1], You Zhou[2], Zhi Gang Yu[4], Ivan I. Kravchenko[5], Dayrl P. Briggs[5], Parikshit Moitra[6], Srini Krishnamurthy[1] and Jason Valentine[3]

[1]Applied Optics Laboratory, SRI International, Menlo Park, CA 94025, USA
[2]Interdisciplinary Materials Science Program, and [3]Department of Mechanical Engineering, Vanderbilt University, Nashville, TN 37212, USA
[4]Institute for Shock Physics, Washington State University, Pullman, WA 99164, USA
[5]Center for Nanophase Materials Sciences, Oak Ridge National Laboratory, Oak Ridge, TN 37831, USA
[6]Optoelectronics Research Centre, University of Southampton, Southampton SO17 1BJ, UK

JV, 0000-0001-9943-7170

Polarization beam splitters, devices that separate the two orthogonal polarizations of light into different propagation directions, are among the most ubiquitous optical elements. However, traditionally polarization splitters rely on bulky optical materials, while emerging optoelectronic and photonic circuits require compact, chip-scale polarization splitters. Here, we show that a rectangular lattice of cylindrical silicon Mie resonators functions as a polarization splitter, efficiently reflecting one polarization while transmitting the other. We show that the polarization splitting arises from the anisotropic permittivity and permeability of the metasurface due to the twofold rotational symmetry of the rectangular unit cell. The high polarization efficiency, low loss and low profile make these metasurface polarization splitters ideally suited for monolithic integration with optoelectronic and photonic circuits.

This article is part of the themed issue 'New horizons for nanophotonics'.

© 2017 The Author(s) Published by the Royal Society. All rights reserved.

1. Introduction

In general, polarizers can be divided into two types: absorptive polarizers and polarization beam splitters. Absorptive polarizers use wire grids, dichroic materials or nanoparticle composites to absorb the rejected polarization [1,2]. Although they provide high degrees of polarization, because the rejected polarization is absorbed, both polarizations cannot be analysed simultaneously. This makes them unsuitable for applications such as optical quantum computing, where polarization splitters are needed to produce quantum bits, or qubits, by dividing single circularly polarized photons into a superposition of vertical and horizontal polarizations [3–6]. Alternatively, polarization beam splitters preserve the rejected polarization by either reflection or diffraction. Commercially available polarization beam splitters separate the polarizations using total internal reflection in birefrigent cubes or Brewster angle reflection in multi-layer dielectric films. While these devices provide efficient polarization splitting, their large profile makes them incompatible with chip-scale photonic and optoelectronic devices [7,8].

Recently, there has been considerable effort to redesign bulky optical elements using metasurfaces [9,10], i.e. planar, subwavelength layers with structural elements designed to modify the amplitude, phase and polarization of scattered light. While originally developed with metallic resonators [11–16], recent studies have shown that dielectric resonators can be used to realize lower absorption loss. Demonstrations of all-dielectric metasurfaces include metasurface reflectors [17–19] and antireflection coatings [20], Fano-resonant surfaces for narrowband spectral filtering [21–23], gradient-phase metasurfaces functioning as spatial-light modulators [24–26] and lenses [27], and periodic arrays of anisotropic (i.e. polarization-dependent) scattering elements functioning as polarizers [28], polarization rotators [24] and converters [22].

Gradient-phase metasurfaces have also been used to design polarization splitters [7,8,29,30]. These function by diffracting the two orthogonal polarizations into different grating modes using periodic binary or multi-level phase gratings with anisotropic unit cells. However, their performance is limited by diffraction efficiency, as some energy is always lost to the specular mode due to diffraction associated with the finite length of the unit cell [7,31]. Alternatively, integrated polarization splitters have been designed for waveguide propagation using genetic algorithms [32], but their efficiencies are low, and the tedious design process is not readily adaptable to different wavelengths or materials.

In contrast to these designs, our polarization splitter derives its properties from an anisotropic permittivity and permeability originating from a rectangular lattice. We showed previously that a subwavelength *square* array of silicon cylinders can reflect more than 99.7% of unpolarized near-infrared light [17,18,33]. Such high reflectivity by a subwavelength layer is achieved by choosing the cylinder size to obtain enhanced backscattering due to electric and magnetic Mie resonances. By breaking the fourfold rotational symmetry of the square lattice, here we show that a *rectangular* lattice with twofold rotational symmetry can be used to make near-infrared beam-splitting polarizers, efficiently reflecting one polarization while transmitting the other. As our polarization splitter operates on the zero-order mode by introducing an effective anisotropic permittivity and permeability through a rectangular lattice, the performance is not limited by diffraction efficiency. Along with particle size, the additional degree of freedom provided by the anisotropic lattice allows independent control of the reflection for the two polarizations, and paves the way for a new class of metasurface polarization elements.

First, we apply our full-wave models (see the electronic supplementary material, S1, §1) to show that a metasurface with a rectangular lattice functions as a polarization splitter. A schematic of the metasurface and the calculated polarization-dependent reflectivity for several rectangular lattices are shown in figure 1. The metasurface consists of a rectangular array of silicon cylinders on a silica substrate. The diameter and height of the cylinders, respectively, are 0.36 μm and 0.46 μm. To study the effects of a rectangular lattice, we fixed the periodicity along x to $a_x = 0.7\,\mu\text{m}$ and increased the periodicity along y (a_y). For the isotropic square lattice with $a_y = a_x$, the reflectivity is equivalent for the two polarizations, with local maxima at 1.55 and 1.3 μm, corresponding to the magnetic and electric Mie resonances, respectively [17,18]. As a_y

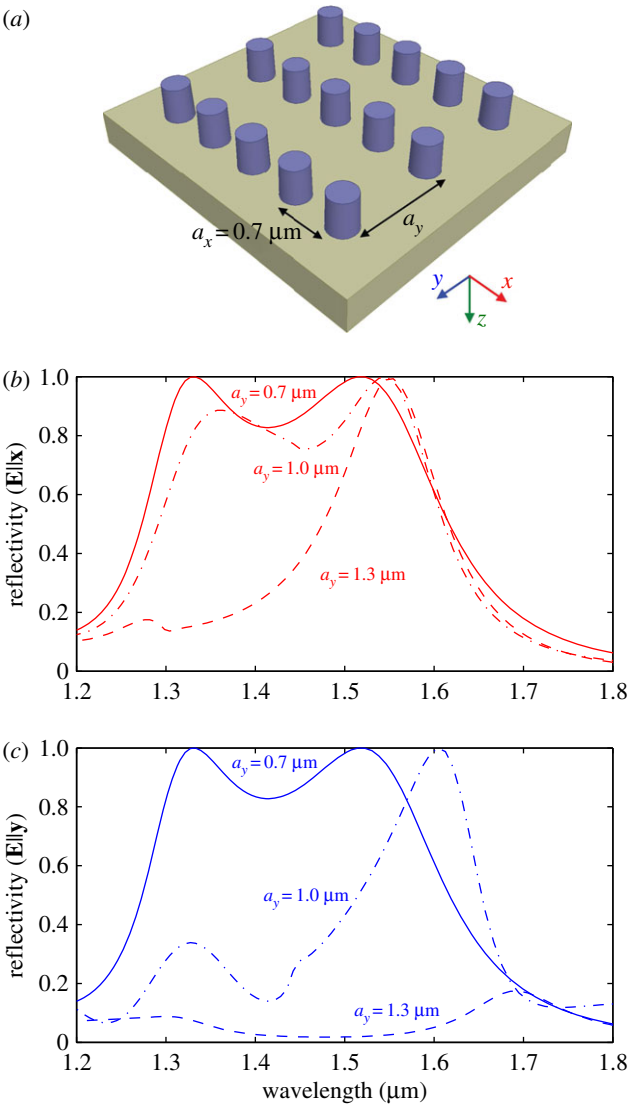

Figure 1. Schematic of the anisotropic metasurface (*a*) and the calculated reflectivity for $a_x = 0.7\ \mu m$ and different values of a_y, for light propagating along *z* and polarized along *x* (*b*) and *y* (*c*). As a_y increases, the reflection maximum due to the electric resonance at 1.3 μm decreases for both polarizations, while the maximum due to the magnetic resonance at 1.55 μm decreases only for **E**||**y**. (Online version in colour.)

increases, the reflectivity at the electric resonance decreases for both polarizations, while the reflectivity at the magnetic resonance decreases only when the electric field is along the long axis of the rectangular unit cell (**E**||**y**). Thus, near the magnetic resonance the metasurface functions as a polarization splitter, efficiently reflecting one polarization while transmitting the other.

The optimal design with $a_y = 1.3\ \mu m$ was selected for fabrication. Figure 2 shows a scanning electron micrograph (SEM) of the fabricated metasurface along with the measured and modelled reflectivity (see the electronic supplementary material, S1, §4). The metasurface was fabricated from polycrystalline silicon (poly-Si) on a silica substrate using electron beam lithography and reactive ion etching (see the electronic supplementary material, S1, §3). From the SEM, the periodicity along *x* and *y*, respectively, is 0.7 and 1.3 μm, and the height, top diameter and bottom diameter are 0.46, 0.35 and 0.37 μm, respectively. At the design wavelength of 1.55 μm,

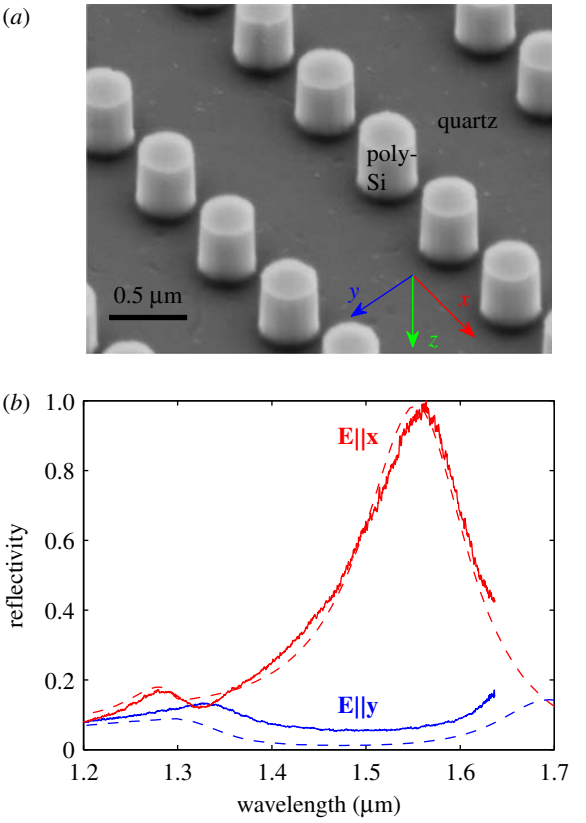

Figure 2. SEM of the metasurface consisting of a rectangular array of poly-Si cylinders on a quartz substrate (*a*) and the measured (solid lines) and modelled (dashed lines) reflectivity for light propagating along *z* and polarized along *x* and *y* (*b*). At 1.55 μm, the anisotropic metasurface efficiently reflects light polarized along *x* while transmitting light polarized along *y*, and thus functions as a polarization splitter. (Online version in colour.)

the predicted reflectivity is greater than 99% for **E**∥**x**, and less than 2% for **E**∥**y**. While the calculated reflectivity for **E**∥**x** is in excellent agreement with the measured value, the apparent discrepancy for **E**∥**y** can be explained by a slight (45 nm) overetch of the cylinders (see the electronic supplementary material, S1, §5). The calculated transmission at 1.55 μm for **E**∥**y**, shown in the electronic supplementary material, S1, §5, is greater than 98%. However, because the periodicity along *y* is larger than the design wavelength in the quartz substrate (1.07 μm), the substrate supports higher-order diffraction modes, namely ±1 orders. We find that a significant fraction (40%) of the transmitted power is diffracted into these higher-order modes (see the electronic supplementary material, S1, §2). However, our models indicate that when the quartz substrate is replaced by porous Si, which does not support higher-order modes due to its low refractive index of 1.1, the zero-order transmission can be greater than 90%.

In contrast to interparticle Bragg scattering in diffraction gratings and photonic crystals, the high reflectivity of our metasurface originates from scattering resonances within the unit cell. This can be seen by analysing the backscattering cross section of the four-particle unit cell, shown in figure 3. We find that the maxima in the backscattering cross section of the unit cell coincide with the maxima in the reflectivity of the array. Noting that the scattering resonances near 1.55 μm and 1.3 μm, respectively, correspond to magnetic and electric modes, we find that only the magnetic mode for **E**∥**x** leads to a cross section considerably larger than the area of the unit cell (0.91 μm^2).

As the cross section is proportional to the scattered field intensity, to understand why only the magnetic mode for **E**∥**x** leads to a large cross section and high reflectivity, we calculated

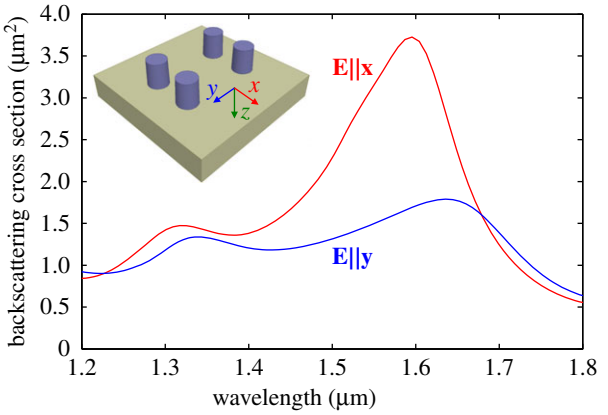

Figure 3. Calculated backscattering cross section of a four-particle unit cell, showing that the reflectivity of the metasurface originates from the polarization-dependent resonant backscattering of the unit cell. (Online version in colour.)

the scattered electric and magnetic field distributions (normalized to the incident fields) at the respective Mie resonance frequencies for both polarizations (figure 4). We find considerable electric field coupling between the cylinders for both polarizations, leading to relatively small field enhancement. On the other hand, the magnetic fields are well confined, particularly for $\mathbf{E}\|\mathbf{x}$. The reason for the varying confinement of the electric and magnetic fields can be traced to their different boundary conditions. As the normal components of $\mathbf{B}$ $(=\mu\mathbf{H})$ and $\mathbf{D}$ $(=\epsilon\mathbf{E})$ must be continuous across the cylinder surface, the normal component of $\mathbf{H}$ is also continuous because $\mu = 1$ throughout, whereas the normal component of $\mathbf{E}$ is discontinuous owing to the large dielectric mismatch between silicon and free space. This leads to a larger normal component of $\mathbf{E}$ just outside the cylinder surface, and hence electric field coupling and poor confinement. Alternatively, the normal component of $\mathbf{H}$ is continuous, leading to better field confinement and less coupling, particularly when the magnetic field is perpendicular to the short axis of the rectangular unit cell (i.e. $\mathbf{E}\|\mathbf{x}$). The large magnetic field enhancement and weak interparticle coupling for $\mathbf{E}\|\mathbf{x}$ leads to a large backscattering cross section and reflectivity at 1.55 μm.

We have shown that the polarization-dependent reflection at 1.55 μm arises from a strong magnetic-dipole Mie resonance for $\mathbf{E}\|\mathbf{x}$ and a redshift and weakening of the magnetic resonance for $\mathbf{E}\|\mathbf{y}$. The polarization-dependent reflection can also be understood in terms of the anisotropic effective parameters of the metasurface. Figure 5*a* and *b*, respectively, shows the real part of the effective permeability (μ) and permittivity (ϵ) for the zero-order mode of the anisotropic metasurface calculated using *S*-parameter inversion (see the electronic supplementary material, S1, §1) [34]. We showed previously that bands of high reflectivity occur where ϵ or μ is negative [33], in contrast to negative index materials, which require both ϵ and μ to be negative. We find that only the magnetic resonance for $\mathbf{E}\|\mathbf{x}$ leads to a negative μ, in this case around 1.55 μm, coinciding with the peak reflectivity in figure 2*b*. At the same wavelength, we find that both ϵ and μ for $\mathbf{E}\|\mathbf{y}$ are close to 1, consistent with the low reflectivity of the metasurface at 1.55 μm for $\mathbf{E}\|\mathbf{y}$. We also note that, in this effective medium description, diffraction in the substrate manifests as effective loss through the imaginary parts of ϵ and μ (not shown).

In summary, we have shown that a rectangular lattice of cylindrical silicon Mie resonators functions as a polarization splitter, efficiently reflecting one polarization while transmitting the other. The polarization-dependent reflection arises from anisotropic near-field coupling between resonators in the rectangular lattice, and can be understood in terms of the anisotropic permittivity and permeability of the metasurface. The polarization efficiency is considerably larger than for devices based on diffraction [29,30] and comparable to commercial polarizing beamsplitter cubes. The high degree of polarization, low loss and low profile of these metasurface

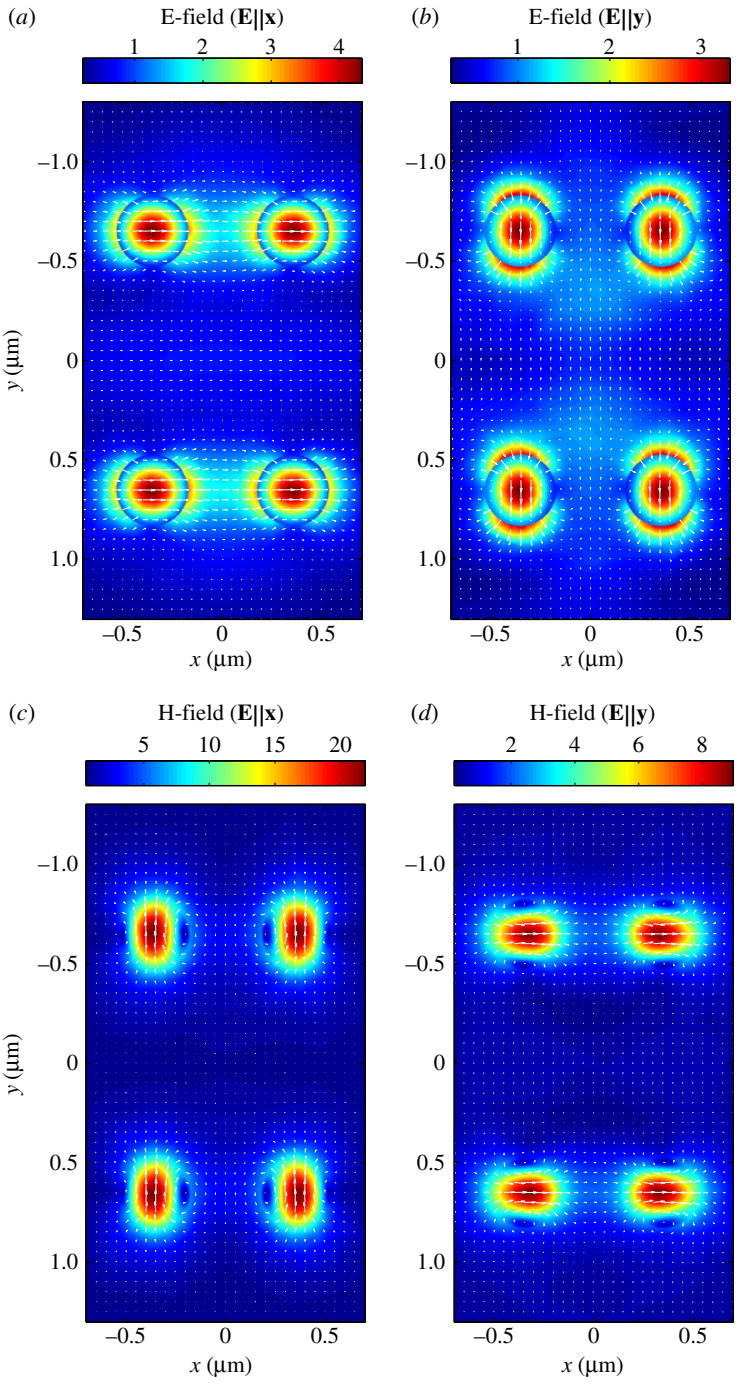

Figure 4. Electric field enhancement at resonance (1.3 μm) for **E**||**x** (*a*) and **E**||**y** (*b*). Magnetic field enhancement at resonance (1.55 μm) for **E**||**x** (*c*) and **E**||**y** (*d*). The electric field is poorly confined for both polarizations, leading to relatively small field enhancement. The magnetic fields are well confined, particularly for **E**||**x**.

polarization splitters may lead to novel designs for integrated photonics and chip-scale optical quantum devices. Most importantly, the introduction of an additional design degree of freedom—the anisotropic lattice—paves the way for a new class of metasurface polarization elements.

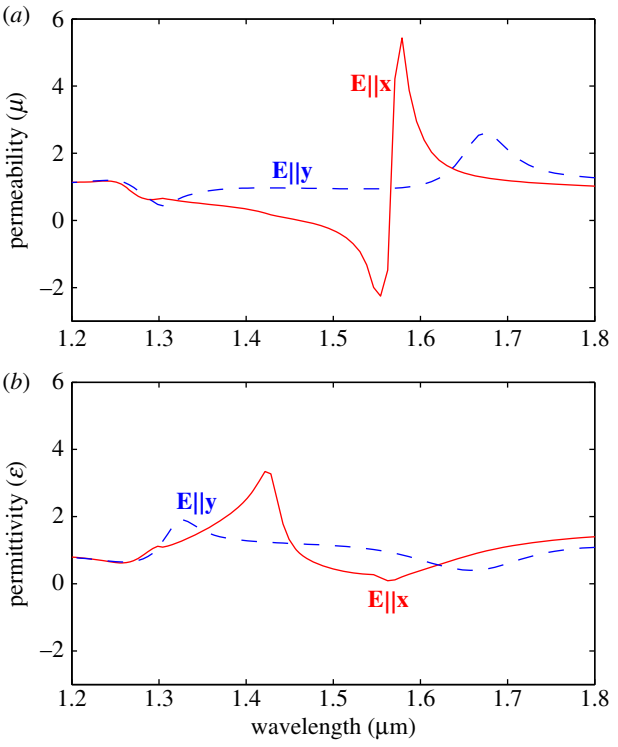

Figure 5. Real part of the effective permeability (*a*) and permittivity (*b*) of the anisotropic metasurface polarization splitter. At 1.55 μm, the magnetic resonance for **E**||**x** leads to negative μ, while both ϵ and μ for **E**||**y** are close to 1. (Online version in colour.)

Competing interests. We declare we have no competing interests.

Funding. This study was financially supported by the Office of Naval Research (ONR) (N00014-12-1-0722, N00014-16-1-2283) and the National Science Foundation (NSF) (ECCS-1351334).

Acknowledgements. A portion of this research was conducted at the Center for Nanophase Materials Sciences, which is a DOE Office of Science User Facility.

References

1. Saleh BEA, Teich MC. 2007 *Fundamentals of photonics*, 2nd edn. New York, NY: Wiley.
2. Nicolais L, Carotenuto G. 2004 *Metal-polymer nanocomposites*. New York, NY: John Wiley & Sons.
3. Pittman TB, Jacobs BC, Franson JD. 2001 Probabilistic quantum logic operations using polarizing beam splitters. *Phys. Rev. A* **64**, 062311. (doi:10.1103/PhysRevA.64.062311)
4. Pan JW, Gasparoni S, Ursin R, Weihs G, Zeilinger A. 2003 Experimental entanglement purification of arbitrary unknown states. *Nature* **423**, 417–422. (doi:10.1038/nature01623)
5. Politi A, Cryan MJ, Rarity JG, Yu S, O'Brien JL. 2008 Silica-on-silicon waveguide quantum circuits. *Science* **320**, 646–649. (doi:10.1126/science.1155441)
6. Gevaux D. 2008 Optical quantum circuits: to the quantum level. *Nat. Photon.* **2**, 337. (doi:10.1038/nphoton.2008.92)
7. Walker SJ, Jahns J, Li L, Mansfield WM, Mulgrew P, Tennant DM, Roberts CW, West LC, Ailawadi NK. 1993 Design and fabrication of high-efficiency beam splitters and beam deflectors for integrated planar micro-optic systems. *Appl. Opt.* **32**, 2494–2501. (doi:10.1364/AO.32.002494)
8. Wang B, Zhou C, Wang S, Feng J. 2007 Polarizing beam splitter of a deep-etched fused-silica grating. *Opt. Lett.* **32**, 1299–1301. (doi:10.1364/OL.32.001299)

9. Kildishev AV, Boltasseva A, Shalaev VM. 2013 Planar photonics with metasurfaces. *Science* **339**, 1232009. (doi:10.1126/science.1232009)
10. Yu N, Capasso F. 2014 Flat optics with designer metasurfaces. *Nat. Mat.* **13**, 139–150. (doi:10.1038/nmat3839)
11. Yu N, Genevet P, Kats MA, Aieta F, Tetienne J-P, Capasso F, Gaburro Z. 2011 Light propagation with phase discontinuities: generalized laws of reflection and refraction. *Science* **334**, 333–337. (doi:10.1126/science.1210713)
12. Ni X, Emani NK, Kildishev AV, Boltasseva A, Shalaev VM. 2012 Broadband light bending with plasmonic nanoantennas. *Science* **335**, 427. (doi:10.1126/science.1214686)
13. Sun S, Yang KY, Wang CM, Juan TK, Chen WT, Liao CY, Zhou L. 2012 High-efficiency broadband anomalous reflection by gradient meta-surfaces. *Nano Lett.* **12**, 6223–6229. (doi:10.1021/nl3032668)
14. Huang L, Chen X, Mühlenbernd H, Li G, Bai B, Tan Q, Jin G, Zentgraf T, Zhang S. 2012 Dispersionless phase discontinuities for controlling light propagation. *Nano Lett.* **12**, 5750–5755. (doi:10.1021/nl303031j)
15. Pors A, Nielsen MG, Eriksen RL, Bozhevolnyi SI. 2013 Broadband focusing flat mirrors based on plasmonic gradient metasurfaces. *Nano Lett.* **13**, 829–834. (doi:10.1021/nl304761m)
16. Aieta F, Genevet P, Kats MA, Yu N, Blanchard R, Gaburro Z, Capasso F. 2012 Aberration-free ultrathin flat lenses and axicons at telecom wavelengths based on plasmonic metasurfaces. *Nano Lett.* **12**, 4932–4936. (doi:10.1021/nl302516v)
17. Moitra P, Slovick BA, Yu ZG, Krishnamurthy S, Valentine J. 2014 Experimental demonstration of a broadband all-dielectric metamaterial perfect reflector. *Appl. Phys. Lett.* **104**, 171102. (doi:10.1063/1.4873521)
18. Moitra P, Slovick BA, Li W, Kravchenko II, Briggs DP, Krishnamurthy S, Valentine J. 2015 Large-scale all-dielectric metamaterial perfect reflectors. *ACS Photon.* **2**, 692–698. (doi:10.1021/acsphotonics.5b00148)
19. Liu S *et al.* 2014 Optical magnetic mirrors without metals. *Optica* **1**, 250. (doi:10.1364/OPTICA.1.000250)
20. Spinelli P, Verschuuren MA, Polman A. 2012 Broadband omnidirectional antireflection coating based on subwavelength surface Mie resonators. *Nat. Commun.* **3**, 692. (doi:10.1038/ncomms1691)
21. Miroshnichenko AE, Kivshar YS. 2012 Fano resonances in all-dielectric oligomers. *Nano Lett.* **12**, 6459–6463. (doi:10.1021/nl303927q)
22. Wu C, Arju N, Kelp G, Fan JA, Dominguez J, Gonzales E, Tutuc E, Brener I, Shvets G. 2014 Spectrally selective chiral silicon metasurfaces based on infrared Fano resonances. *Nat. Commun.* **5**, 3892. (doi:10.1038/ncomms4892)
23. Zhang J, MacDonald KF, Zheludev NI. 2013 Near-infrared trapped mode magnetic resonance in an all-dielectric metamaterial. *Opt. Express* **21**, 26721. (doi:10.1364/OE.21.026721)
24. Yang Y, Wang W, Moitra P, Kravchenko II, Briggs DP, Valentine J. 2014 Dielectric meta-reflectarray for broadband linear polarization conversion and optical vortex generation. *Nano Lett.* **14**, 1394–1399. (doi:10.1021/nl4044482)
25. Chong KE *et al.* 2015 Polarization-independent silicon metadevices for efficient optical wavefront control. *Nano Lett.* **15**, 5369–5374. (doi:10.1021/acs.nanolett.5b01752)
26. Lin D, Fan P, Hasman E, Brongersma ML. 2014 Dielectric gradient metasurface optical elements. *Science* **345**, 298–302. (doi:10.1126/science.1253213)
27. Aieta F, Kats MA, Genevet P, Capasso F. 2015 Multiwavelength achromatic metasurfaces by dispersive phase compensation. *Science* **347**, 1342–1345. (doi:10.1126/science.aaa2494)
28. Shen B, Wang P, Polson R, Menon R. 2014 Ultra-high-efficiency metamaterial polarizer. *Optica* **1**, 356. (doi:10.1364/OPTICA.1.000356)
29. Zheng J, Ye ZC, Sun NL, Zhang R, Sheng ZM, Shieh HPD, Zhang J. 2014 Highly anisotropic metasurface: a polarized beam splitter and hologram. *Sci. Rep.* **4**, 6491. (doi:10.1038/srep06491)
30. Arbabi A, Horie Y, Bagheri M, Faraon A. 2015 Dielectric metasurfaces for complete control of phase and polarization with subwavelength spatial resolution and high transmission. *Nat. Nanotechnol.* **10**, 937–943. (doi:10.1038/nnano.2015.186)
31. Suleski TJ, Kathman AD, Prather DW. 2004 *Diffractive optics: design, fabrication, and test*. Bellingham, WA: SPIE Press.

32. Shen B, Wang P, Polson R, Menon R. 2015 An integrated-nanophotonics polarization beamsplitter with $2.4 \times 2.4\,\mu m^2$ footprint. *Nat. Photon.* **9**, 378–382. (doi:10.1038/nphoton.2015.80)
33. Slovick B, Yu ZG, Berding M, Krishnamurthy S. 2013 Perfect dielectric-metamaterial reflector. *Phys. Rev. B* **88**, 165116. (doi:10.1103/PhysRevB.88.165116)
34. Smith DR, Schultz S, Markoš P, Soukoulis CM. 2012 Determination of effective permittivity and permeability of metamaterials from reflection and transmission coefficients. *Phys. Rev. B* **65**, 195104. (doi:10.1103/PhysRevB.65.195104)